Proceedings, Bicycle and Motorcycle Dynamics 2010
Symposium on the Dynamics and Control of Single Track Vehicles,
20–22 October 2010, Delft, The Netherlands

Automatic Generation of Linearised Equations of Motion for Moving Vehicles

B.P. Minaker

Department of Mechanical, Automotive, & Materials Engineering
University of Windsor
401 Sunset Avenue, Windsor ON N9B 3P4, Canada
e-mail: bminaker@uwindsor.ca

ABSTRACT

This paper demonstrates a method for automatic generation of the linearised equations of motion for mechanical systems. Unlike conventional methods for generating linearised equations of motion in 'MCK' form, the method allows for the analysis of systems with nonholonomic constraints, and allows linearisation around non-zero speeds. With this method, the algebraic constraint equations are eliminated after the linearisation while the resulting system is already written in first order form. The method has been successfully applied to an assortment of problems of varying complexity. It has been implemented in the MATLAB®/Octave programming language, under the title 'EoM', and is freely available under the GNU General Public License on the author's website. It can easily generate eigenvalue or frequency response plots for a number of systems of interest to the vehicle analyst.

1 INTRODUCTION

There are many approaches to generating equations of motion for mechanical systems, and each has its advantages; this paper describes a particular method that is of interest as it is well suited to vehicle stability analysis. The method is distinguished by the manner in which the constraint equations are eliminated. When using this approach, the resulting linearised equations of motion never appear in the traditional linear second order form; instead, the kinematic differential equations are utilized to arrive at a first order form before the constraints are eliminated. The method is well suited for vehicle stability, as it easily accommodates both nonholonomic constraints, and linearisation around non-zero speed equilibrium points.

2 DEVELOPMENT

2.1 Kinematic Differential Equations, Newton-Euler equations

The foundation of the method is the linearised Newton-Euler equations, combined with the linearised kinematic differential equations, as given in Equation (1). The equations of motion are written in physical coordinates, representing the location of each bodies' centre of mass, and the orientation of a body fixed reference frame. The positions and orientations ($\boldsymbol{p}$) are expressed in a fixed global frame, where the velocities and angular velocities ($\boldsymbol{w}$) are given in the body fixed moving reference frame. The orientations are assumed to be small angles, allowing representation as a three coordinate orientation vector. Combining the equations in this fashion results in a first order form.

$$\begin{bmatrix} \mathbf{I} & \mathbf{0} \\ \mathbf{0} & \mathbf{M} \end{bmatrix} \begin{Bmatrix} \dot{\boldsymbol{p}} \\ \dot{\boldsymbol{w}} \end{Bmatrix} + \begin{bmatrix} \mathbf{V} & -\mathbf{I} \\ \mathbf{K} & \mathbf{C} \end{bmatrix} \begin{Bmatrix} \boldsymbol{p} \\ \boldsymbol{w} \end{Bmatrix} = \begin{Bmatrix} 0 \\ \boldsymbol{f}_{\mathrm{c}} + \boldsymbol{f}_{\mathrm{a}} \end{Bmatrix} \tag{1}$$

The motion at equilibrium is assumed to be composed of a translation component, and a rotation component. Of course, any large rotational speed at equilibrium would violate the assumption of small orientation angles. Non-zero angular speeds at the point of linearisation are accommodated by allowing rotation around an axisymmetric axis, relative to the moving reference frame. In this case, the orientation angles represent the orientation of the reference frame, rather than the body itself. The $\mathbf{V}$ matrix resulting from the linearisation of the kinematic differential equations contains the skew symmetric matrix of the translational velocities of the bodies, arranged in the upper right 3x3 sub-matrix of the set of 6x6 matrices arranged along the diagonal. All other entries are zero. The $\mathbf{C}$ matrix contains the traditional viscous damping matrix, plus terms due to the inertia forces, i.e., centripetal forces and gyroscopic moments. The stiffness matrix $\mathbf{K}$ is the sum of terms resulting from deflection of elastic elements, and additional tangent stiffness matrix terms. The mass matrix $\mathbf{M}$ results from Newton's Laws, and is tri-diagonal as is typical. The externally applied and constraint forces appear in the right hand side. For further details on the derivation of the equations, see Minaker and Rieveley[1].

As mentioned above, the stiffness matrices used include a number of tangent stiffness terms, i.e., terms resulting from preloads or other forces acting in the system. The tangent stiffness terms are key to capturing the tilting behaviour of bicycles or motorcycles. The total stiffness matrix of a body acted on by a typical linear spring, given in Equation (2), is built from three terms. Only the first term depends on the stiffness of the spring, while the tangent stiffness terms depend on the preload and the length. In this case, these terms physically represent the change in direction of the constant magnitude spring preload force, and the change in applied moment due to the change in location relative to the centre of mass.

$$\mathbf{K} = \begin{bmatrix} \boldsymbol{u} \\ \tilde{\boldsymbol{r}}\boldsymbol{u} \end{bmatrix} k \begin{bmatrix} \boldsymbol{u}^{\mathrm{T}} & (\tilde{\boldsymbol{r}}\boldsymbol{u})^{\mathrm{T}} \end{bmatrix} + \begin{bmatrix} \tilde{\boldsymbol{u}} \\ \tilde{\boldsymbol{r}}\tilde{\boldsymbol{u}} \end{bmatrix} \frac{f}{l} \begin{bmatrix} \tilde{\boldsymbol{u}}^{\mathrm{T}} & (\tilde{\boldsymbol{r}}\tilde{\boldsymbol{u}})^{\mathrm{T}} \end{bmatrix} - \begin{bmatrix} \mathbf{0} & \mathbf{0} \\ \mathbf{0} & \tilde{\boldsymbol{F}}\tilde{\boldsymbol{r}} \end{bmatrix} \tag{2}$$

The stiffness of the spring is k, the preload is f, and the length, as loaded, is l. The unit vector u gives the direction of the spring, and the vector r gives the location of the endpoint of the spring, relative to the centre of mass of the body to which it is attached. The tilde operator indicates the skew symmetric matrix.

In order to find the complete stiffness matrix, all forces acting at the point of linearisation, and their corresponding tangent stiffness terms, must be considered; even terms due to constant applied forces or internal constraint forces must be included. For example, a constant applied force-moment pair has the following stiffness matrix:

$$\mathbf{K} = - \begin{bmatrix} \mathbf{0} & \mathbf{0} \\ \mathbf{0} & \tilde{\boldsymbol{F}}\tilde{\boldsymbol{r}} \end{bmatrix} + \frac{1}{2} \begin{bmatrix} \mathbf{0} & \mathbf{0} \\ \mathbf{0} & \tilde{\boldsymbol{M}} \end{bmatrix} \tag{3}$$

In the author's implementation, externally applied moments are considered to be 'cross semi-tangential', using the terminology of Ritto-Corrêa and Camotim[2], meaning that they could be effectively reproduced using two pairs of equal and opposite forces that are fixed in magnitude and direction, where the directions of the two pairs are orthogonal. This assumption results in the somewhat unexpected factor of one half appearing.

2.2 Constraint Equations

Constraints are imposed through a set of six equations. Because the positions and velocities are given as separate states, the holonomic constraint equations are applied twice; first in their original form, and again, in differentiated form. The choice of coordinates results in repetition of the coefficients when the constraints are applied to the state vector of global position/local velocity, and when they are applied to the derivative of the state vector, (i.e., global velocity/local acceleration). There is some redundancy in the constraints at the velocity level, due to the way the kinematic differential equations are incorporated. However, this redundancy does not influence the number or type of the final set of coordinates, and thus does not pose a problem. Nonholonomic constraints are applied to velocity and acceleration only. The combined constraint equations are given in Equation (4), where the $\mathbf{B}_{\mathrm{h}}$ and $\mathbf{B}_{\mathrm{nh}}$ matrices represent the holonomic and nonholonomic constraint equations, respectively.

$$\begin{bmatrix} \mathbf{B}_{\mathrm{h}} & \mathbf{0} \\ -\mathbf{B}_{\mathrm{h}}\mathbf{V} & \mathbf{B}_{\mathrm{h}} \\ \mathbf{0} & \mathbf{B}_{\mathrm{nh}} \end{bmatrix} \begin{bmatrix} \dot{\boldsymbol{p}} & \boldsymbol{p} \\ \dot{\boldsymbol{w}} & \boldsymbol{w} \end{bmatrix} = \begin{bmatrix} \mathbf{0} & \mathbf{0} \\ \mathbf{0} & \mathbf{0} \\ \mathbf{0} & \mathbf{0} \end{bmatrix} \tag{4}$$

In order to eliminate the constraint equations, a new state vector $\boldsymbol{z}$ that will always satisfy the constraints is defined, using an orthogonal complement $\mathbf{R}$. The orthogonal complement is not unique, and depends on the method used for its evaluation. In the author's implementation, the standard null space routines in MATLAB, which are based on a singular value decomposition approach, are used.

$$\begin{Bmatrix} \boldsymbol{p} \\ \boldsymbol{w} \end{Bmatrix} = \mathbf{R}\boldsymbol{z} \;\middle|\; \begin{bmatrix} \mathbf{B}_{\mathrm{h}} & \mathbf{0} \\ -\mathbf{B}_{\mathrm{h}}\mathbf{V} & \mathbf{B}_{\mathrm{h}} \\ \mathbf{0} & \mathbf{B}_{\mathrm{nh}} \end{bmatrix} \mathbf{R} = \mathbf{0} \Rightarrow \begin{bmatrix} \mathbf{B}_{\mathrm{h}} & \mathbf{0} \\ -\mathbf{B}_{\mathrm{h}}\mathbf{V} & \mathbf{B}_{\mathrm{h}} \\ \mathbf{0} & \mathbf{B}_{\mathrm{nh}} \end{bmatrix} \begin{Bmatrix} \boldsymbol{p} \\ \boldsymbol{w} \end{Bmatrix} = \begin{Bmatrix} \mathbf{0} \\ \mathbf{0} \\ \mathbf{0} \end{Bmatrix} \tag{5}$$

To reduce the equations to a minimal dimension, and eliminate the forces of constraint, the matrix $\mathbf{L}$ is formed from the sub-matrices $\mathbf{L}_{\mathrm{u}}$ and $\mathbf{L}_{\mathrm{l}}$.

$$\mathbf{L} = \begin{bmatrix} \mathbf{L}_{\mathrm{u}} & \mathbf{0} \\ \mathbf{0} & \mathbf{L}_{\mathrm{l}} \end{bmatrix} \;\middle|\; \mathbf{B}_{\mathrm{h}}\mathbf{L}_{\mathrm{u}} = \mathbf{0} \;\wedge\; \begin{bmatrix} \mathbf{B}_{\mathrm{h}} \\ \mathbf{B}_{\mathrm{nh}} \end{bmatrix} \mathbf{L}_{\mathrm{l}} = \mathbf{0} \Rightarrow \mathbf{L}^{\mathrm{T}} \begin{Bmatrix} \mathbf{0} \\ \boldsymbol{f}_{\mathrm{c}} \end{Bmatrix} = \begin{Bmatrix} \mathbf{0} \\ \mathbf{0} \end{Bmatrix} \tag{6}$$

The resulting first order form is shown in Equation 7. From here, the equations can easily be manipulated into the standard form for eigenvalue or frequency response analysis.

$$\mathbf{L}^{\mathrm{T}} \begin{bmatrix} \mathbf{I} & \mathbf{0} \\ \mathbf{0} & \mathbf{M} \end{bmatrix} \mathbf{R}\dot{\boldsymbol{z}} + \mathbf{L}^{\mathrm{T}} \begin{bmatrix} \mathbf{V} & -\mathbf{I} \\ \mathbf{K} & \mathbf{C} \end{bmatrix} \mathbf{R}\boldsymbol{z} = \mathbf{L}^{\mathrm{T}} \begin{Bmatrix} \mathbf{0} \\ \boldsymbol{f}_{\mathrm{c}} + \boldsymbol{f}_{\mathrm{a}} \end{Bmatrix} \tag{7}$$

3 SIMULATION RESULTS

3.1 Eigenvalues

The results produced have been verified against a number of benchmark problems from the literature, such as the rolling wheel (r=0.5 m) illustrated in Greenwood[3], the Meijaard *et. al.* rigid-rider bicycle[4], and the Ellis truck and trailer[5], as shown in Figure 1. The presence of unstable or oscillatory motions are predicted as expected.

Additionally, the method has been applied to a bicycle and trailer combination; again, results are shown in Figure 1. The bicycle used with the trailer for the model was the previously mentioned benchmark, and the trailer was modelled as a rigid body, attached to the bike by spherical joint, rolling on two wheels, each identical to the rear wheel of the bicycle. The properties of trailer are given in Table 1, using the coordinate system from the benchmark. The results follow that of the reference bicycle closely, with the addition of two non-oscillatory roots, one increasingly stable with speed, one very slightly unstable over the entire speed range.

The method has also been successfully applied to an atypical three wheeled tilting vehicle in Minaker and Rieveley[1]. By varying the parameters of the tilting vehicle suspension, under the direction of a genetic search algorithm, a configuration that stabilises the vehicle over a large range of speeds was found. An eigenvector 'masking' approach was used to ensure that the genetic search algorithm focused its efforts on motions that were predetermined to be more important.

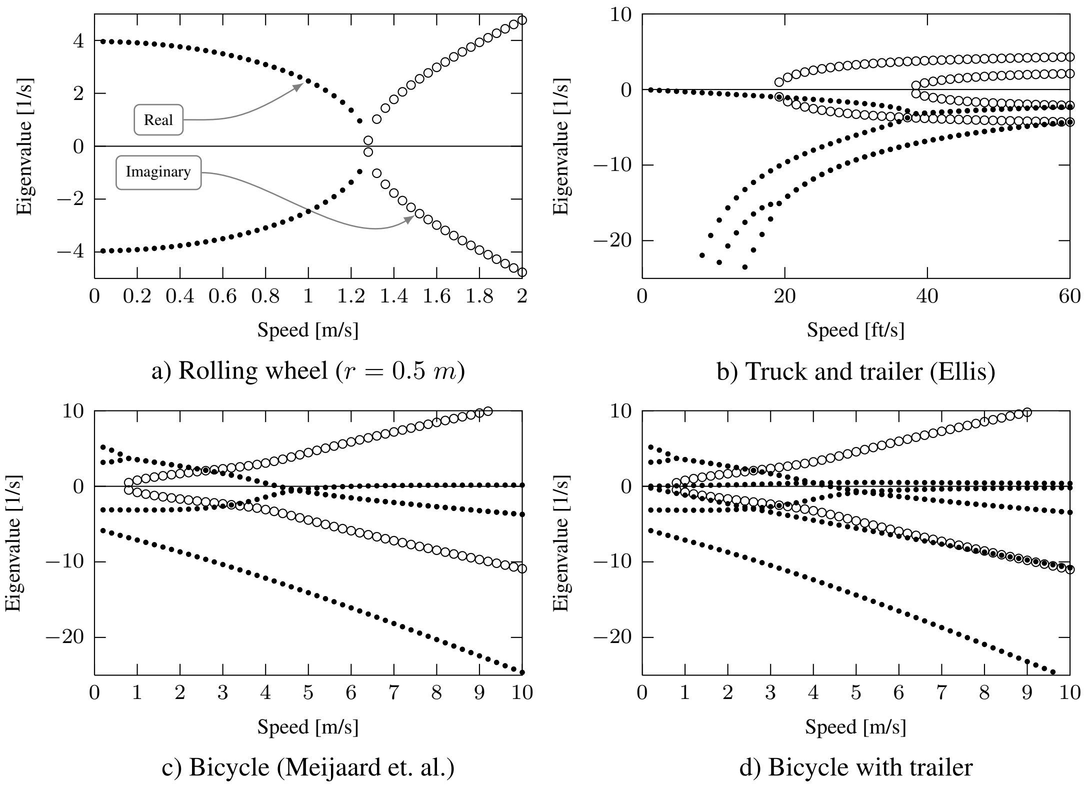

a) Rolling wheel ($r = 0.5\ m$)

b) Truck and trailer (Ellis)

c) Bicycle (Meijaard et. al.)

d) Bicycle with trailer

Figure 1. Eigenvalues vs. speed

Table 1. Trailer parameters

mass	15 [kg]	centre of mass	-0.75,0,-0.4 [m]	tow hitch	0,0,-0.3 [m]
I_{xx}, I_{yy}, I_{zz}	1,1,3 [kg·m^2]	left wheel	-0.9,-0.3,-0.3 [m]		
I_{xy}, I_{yz}, I_{zx}	0,0,0 [kg·m^2]	right wheel	-0.9,0.3,-0.3 [m]		

3.2 Frequency Response

The addition of modelled input actuators, and sensor outputs has allowed the method to be used to compute the frequency response function for a number of complex systems. Of particular interest is the effect of the forward speed on the sensitivity of vehicle systems.

In Figure 2, two Bode plots are given for the Meijaard *et. al.* benchmark bicycle[4]. The first relates the effect of speed and frequency on the yaw rate to steer torque relationship, while the second examines the roll angle. From both plots, it appears that the benchmark bicycle encounters a region of increased low frequency sensitivity at speeds near 6 m/s, and smaller high frequency region of moderately increased sensitivity, at speeds near 4 m/s and frequencies near 1 rad/s. Both the yaw rate and roll angle response drop off considerably at frequencies above 10 rad/s, independent of speed.

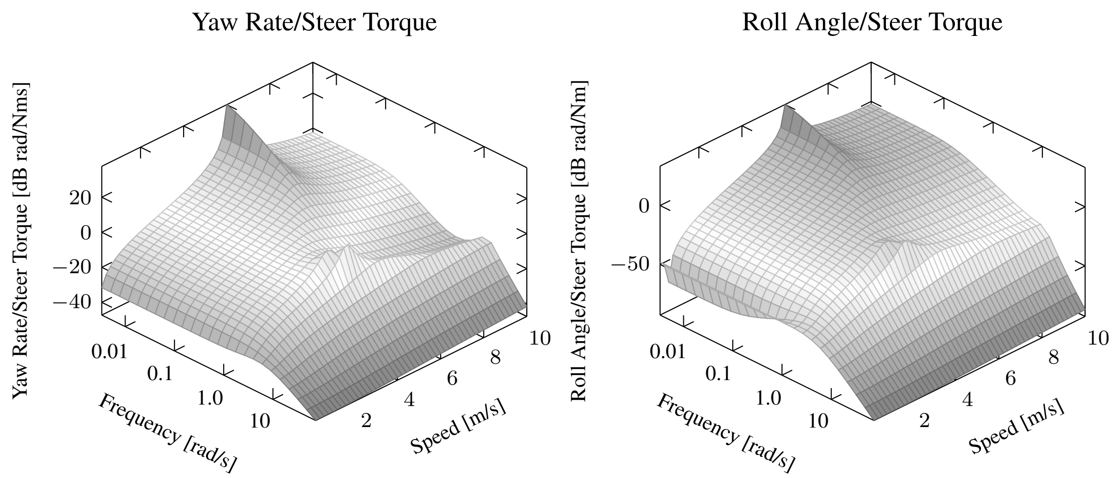

Figure 2. Speed Dependent Bode Plots of Bicycle

4 CONCLUSIONS

The method described has proven to be both a powerful and flexible tool in analysing a number of complex vehicle systems. The linear form of the generated equations makes the method ideal for control systems development, and incorporation of automatic state observer and feedback gain matrices are currently under investigation. In addition, future work will focus on expansion of the library of tangent stiffness matrices for various type of rigid mechanical connections, as well beam or shear panel type springs.

REFERENCES

[1] B.P. Minaker, R.J. Rieveley, "Automatic generation of the non-holonomic equations of motion for vehicle stability analysis", *Vehicle System Dynamics*, vol. 48, no. 9, (2010), pp. 1043–1063.

[2] Manuel Ritto-Corrêa, Dinar Camotim, "Work-conjugacy between rotation-dependent moments and finite rotations", *International Journal of Solids and Structures* 40 (2003), pp. 2851–2873.

[3] D.T. Greenwood, *Principles of Dynamics*, Prentice-Hall, Englewood Cliffs, NJ, 1965.

[4] J.P. Meijaard, J.M. Papadopoulos, A. Ruina, and A.L. Schwab, "Linearised dynamics equations for the balance and steer of a bicycle: a benchmark and review", *Proc. Roy. Soc. A*, 463 (2007), pp. 1955–1982.

[5] J.R. Ellis, *Vehicle Dynamics*, Business Books, London, 1968.